Physics Letters B 710 (2012) 623–629

Contents lists available at SciVerse ScienceDirect

Physics Letters B

www.elsevier.com/locate/physletb

Coupling reduction and the Higgs mass

N.D. Tracas [a,*], G. Tsamis [a], N.D. Vlachos [b], G. Zoupanos [a,c,d]

[a] Physics Department, National Technical University, GR-157 73 Athens, Greece
[b] Theoretical Physics Division, Aristotle University, GR-54124 Thessaloniki, Greece
[c] Max-Planck-Institut für Physik, Föhringer Ring 6, 80805 München, Germany
[d] Arnold-Sommerfeld-Center für Theoretische Physik, Department für Physik, Ludwig-Maximilians-Universität München, Theresienstrasse 37, 80333 München, Germany

ARTICLE INFO

Article history:
Received 26 November 2011
Received in revised form 11 February 2012
Accepted 7 March 2012
Available online 9 March 2012
Editor: G.F. Giudice

ABSTRACT

Assuming the existence of a functional relation among the Standard Model (SM) gauge couplings α_1 and quartic λ, we determine the mass of the Higgs particle. Similar considerations for the top and bottom Yukawa couplings in the minimal supersymmetric SM lead to the prediction of a narrow window for $\tan\beta$, one of the main parameters that determine the light Higgs mass.

1. Introduction

Copious theoretical efforts to establish a deeper understanding of Nature, led to very interesting constructions such as Superstring Theories that aim to unify consistently all interactions. The main goal expected from a unified description of interactions by the Particle Physics community is to understand the present day large number of free parameters of the Standard Model (SM) in terms of a few fundamental ones. Realistically, one expects to achieve at least a partial *reduction of couplings*. Indeed, the celebrated SM had so far outstanding successes in all its confrontations with experimental results. However, its apparent success is spoiled by the presence of a plethora of free parameters mostly related to the ad-hoc introduction of the Higgs and Yukawa sectors in the theory.

Towards reducing the independent parameters of the theory, a method has been developed which looks for renormalization group invariant (RGI) relations [1–9,11] holding below the Planck scale, which in their turn are preserved down to Grand Unified (GUT) or lower scales. This program applied to dimensionless couplings of supersymmetric GUTs, such as gauge and Yukawa couplings, had already noticeable success by predicting correctly, among other things, the top quark mass in the finite and in the minimal $N = 1$ supersymmetric SU(5) GUTs [1,2]. An interesting prediction of the lightest Higgs mass in a $N = 1$ finite SU(5) GUT [1] will soon confront the experiment. An impressive aspect of the RGI relations is that one can guarantee their validity to all orders in perturbation theory by studying the uniqueness of the resulting relations at one loop, as it was proven in the early days of the couplings reduction program [5]. Even more remarkable is the fact that it is possible to find RGI relations among couplings that guarantee finiteness to all orders in perturbation theory [9] (see also [10]). Here, we would like to examine to which extent the above method can be applied to minimal schemes such as the SM and its minimal supersymmetric extension, the MSSM. In fact, the former, was one of the first applications of the above reduction scheme [6,8,11] assuming a perturbative ansatz. The implications of a stronger condition were examined in Ref. [12].

Let us first recall some basic issues concerning the reduction of couplings. A RGI relation $\Phi(g_1, \ldots, g_N) = 0$, has to satisfy the partial differential equation $\mu\, d\Phi/d\mu = \sum_{i=1}^{N} \beta_i \partial\Phi/\partial g_i = 0$, where β_i is the β-function of g_i. There exist $(N-1)$ independent Φ's, and finding the complete set of these solutions is equivalent to solve the so-called reduction equations (REs), $\beta_g(dg_i/dg) = \beta_i$, $i = 1, \ldots, N$, where g and β_g are the primary coupling and its β-function correspondingly. Using all the $(N-1)\Phi$'s to impose RGI relations, one can, in principle, express all the couplings in terms of a single coupling g. The complete reduction, which formally preserves perturbative renormalizability, can be achieved by demanding a power series solution, where its uniqueness can be investigated at the 1-loop level. The completely reduced theory contains only one independent coupling with the corresponding β-function. This possibility of coupling unification is attractive, but it can be too restrictive and hence unrealistic. To overcome this problem, one may use fewer Φ's as RGI constraints.

After investigating specific examples, it becomes clear that the various couplings in supersymmetric theories have easily the same asymptotic behavior. Therefore, searching for a power series solution to the RGEs is justified. This is not the case in non-supersymmetric theories. Still, in the SM α_3 and α_2 have the same behavior but one cannot be reduced in favor of the other [11].

* Corresponding author.
E-mail address: ntrac@central.ntua.gr (N.D. Tracas).

0370-2693
doi:10.1016/j.physletb.2012.03.016

Here, we will examine in some detail the possibility to reduce the couplings α_1 and the scalar quartic coupling λ of the SM, which have the same asymptotic behavior too.

As already mentioned, the method of reduction was applied in the couplings of the SM in Refs. [6,8,11]. The predictions for the Higgs boson mass given in Refs. [6,8] and for the Higgs and the top quark masses in Ref. [11] did not survive confrontation with experiment. In the present work, after studying the evolution of the SM couplings under the renormalization group flow, we look for solutions of the reduction equations following Refs. [1–5,8,9,11] by generalizing their perturbative ansatz. Eventually, we are led to the updated solutions of Ref. [6]. Although exact reduction cannot be realized, numerical investigations show that an approximate reduction still holds especially for the high energy region. Therefore, we will try to further investigate this interesting property both semi-analytically and numerically, and use it to predict the Higgs mass. Our results suggest a Higgs running (pole) mass ~ 163 (155) GeV, i.e. in a region that is currently under experimental investigation, which we do not consider as totally conclusive yet.

If the experimental results persist as in [13] when better statistics are available, then we will consider the SM case as an educative example and a motivation for applying our method to the MSSM, which is examined here too.

2. Studies of the behavior of the couplings under RGEs

In the following, we will investigate the behavior of the SM and MSSM couplings under the renormalization group equations in order to establish a possible realization of the reduction scenario. The most promising case appears to connect the scalar quartic coupling λ and the U(1) gauge coupling α_1. We expect that such a relation leads to a prediction for the Higgs mass. Let us start with the 1-loop contributions. At this level, the RGEs for the gauge and the (top) Yukawa[1] can be solved analytically. The running of the quartic coupling is governed by the equation

$$\frac{d\tilde{\lambda}}{dt} = \beta_\lambda = \frac{1}{2\pi}\big[L_2\tilde{\lambda}^2 + (A_{1L}\alpha_1 + A_{2L}\alpha_2)\tilde{\lambda} + A_{11}\alpha_1^2 + A_{12}\alpha_1\alpha_2 + A_{22}\alpha_2^2 + H_L\alpha_t\tilde{\lambda} + H_2\alpha_t^2\big], \tag{1}$$

where

$$\tilde{\lambda} = \frac{\lambda}{4\pi}, \qquad \alpha_t = \frac{h_t^2}{4\pi}, \qquad t = \ln(E),$$
$$L_2 = 6, \qquad A_{1L} = -\frac{3}{2}, \qquad A_{2L} = -\frac{9}{2},$$
$$A_{11} = \frac{3}{8}, \qquad A_{12} = \frac{3}{4}, \qquad A_{22} = \frac{9}{8}, \qquad H_L = 6, \qquad H_2 = -6,$$

and α_i, $i = 1, 2, 3$ are the gauge couplings.

To check that the ratio λ over α_1 indeed tends to a constant value at high scales, we plot the derivative of the ratio $\eta_\lambda \equiv \tilde{\lambda}/\alpha_1$ as a function of t, for several initial values of the $\tilde{\lambda}$ coupling, which we trade for the (running) Higgs mass. In Fig. 1 we show such a plot. Starting from $m_H = 165$ GeV, we see that the derivative is positive for high energies. Upon lowering the Higgs mass, the derivative decreases and, for $m_H \sim 162$ GeV, it goes asymptotically to zero. Further lowering the Higgs mass the derivative becomes negative but again for $m_H \sim 151.5$ GeV goes once more asymptotically to zero. For even smaller values of the Higgs mass the derivative becomes positive but now $\tilde{\lambda}$ passes through negative

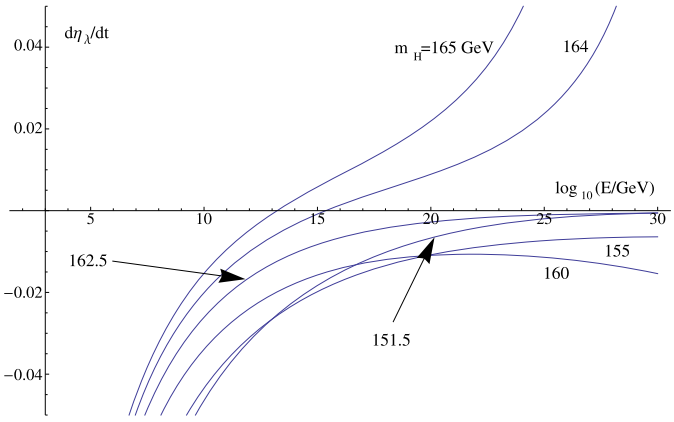

Fig. 1. Plotting the derivative $d\eta_\lambda/dt$ as a function of t.

values.[2] Notice that η_λ becomes constant at energies well above the Planck scale, however at the 2-loop order the situation improves appreciably. Let us explore the above situation a bit further. We can easily express the running of the ratio η_λ in the form

$$\frac{d\eta_\lambda}{dt} = \frac{1}{\alpha_1}\frac{d\tilde{\lambda}}{dt} - \frac{\tilde{\lambda}}{\alpha_1^2}\frac{d\alpha_1}{dt} = \frac{1}{\alpha_1}\beta_\lambda(\alpha_1, \alpha_2, \alpha_t, \tilde{\lambda}) - \frac{\tilde{\lambda}}{\alpha_1^2}\beta_1(\alpha_1), \tag{2}$$

where β_1 is the 1-loop β-function for the α_1 coupling. This expression can be easily cast in the following form

$$\frac{d\eta_\lambda}{dt} = \alpha_1\beta_\lambda(1, \alpha_2/\alpha_1, \alpha_t/\alpha_1, \eta_\lambda) - \alpha_1\eta_\lambda b_1 \tag{3}$$

where $\beta_1 = b_1\alpha_1^2$. Since at the 1-loop level the differential equations for the gauge and Yukawa couplings can be solved independently of the $\tilde{\lambda}$ coupling, we can express α_1, α_2 and α_t as functions of t and recast the above equation in the form

$$\frac{d\eta_\lambda}{dt} = \alpha_1(t)\beta_\lambda(t, \eta_\lambda) - \alpha_1(t)\eta_\lambda\beta_1(1) \equiv \alpha_1(t)F_{\eta_\lambda}(t, \eta_\lambda), \tag{4}$$

using the same symbol β_λ for the new function of t and η_λ. In Fig. 2 we plot contours of constant value (-0.01, 0 and 0.01) for $\alpha_1(t)F_{\eta_\lambda}(t, \eta_\lambda)$ in the (t, η_λ) plane. We clearly see that the zero value contour tends, for albeit very high energies, to a constant value for the ratio η_λ (~ 1.3 and ~ 0.05).

Let us now adopt a different point of view and treat α_1, $\alpha_2/\alpha_1 \equiv \eta_2$, $\alpha_t/\alpha_1 \equiv \eta_t$ and η_λ as independent variables. Then we rewrite Eq. (3) in the form

$$\frac{d\eta_\lambda}{dt} = \alpha_1 F_{\eta_\lambda}(\eta_2, \eta_t, \eta_\lambda) \tag{5}$$

using again the same symbol F_{η_λ}. The derivative of η_λ with respect to α_1 is given by

$$\frac{d\eta_\lambda}{d\alpha_1} = \frac{\frac{d\eta_\lambda}{dt}}{\frac{d\alpha_1}{dt}} = \frac{\alpha_1 F_{\eta_\lambda}(\eta_2, \eta_t, \eta_\lambda)}{b_1\alpha_1^2} = \frac{F_{\eta_\lambda}(\eta_2, \eta_t, \eta_\lambda)}{b_1\alpha_1}. \tag{6}$$

If η_λ tends to a constant value, then the above derivative should tend to zero. This is of course true when α_1 becomes very large but also when the numerator, $F_{\eta_\lambda}(\eta_2, \eta_t, \eta_\lambda)$ is equal to zero. Just to have a first impression, we put $\eta_2 = \eta_t = 0$ (both ratios tend

[1] Only the top Yukawa coupling is taken into account in the running.

[2] Recall that the assumption the λ stays always positive, for the whole energy scale, gives a lower bound to the Higgs mass ~ 149 GeV.

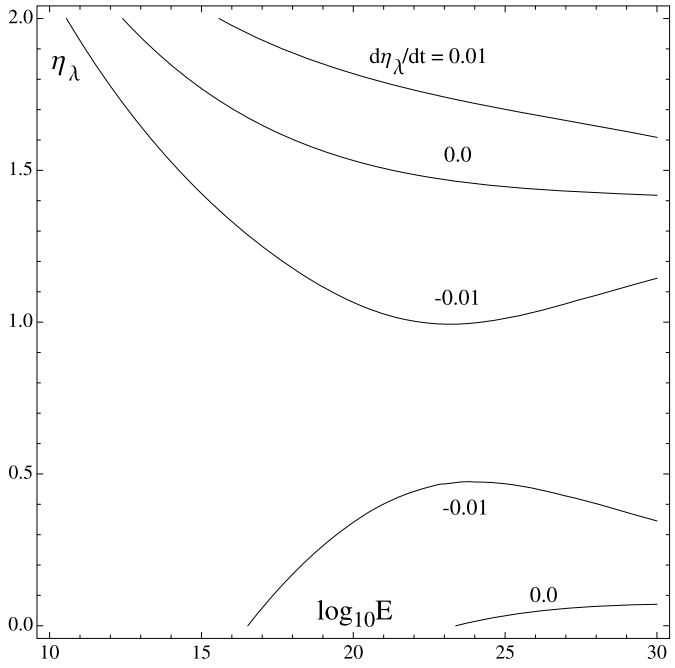

Fig. 2. Contours of constant value of the derivative $d\eta_\lambda/dt$ in the (t, η_λ) plane for three values: -0.01, 0 and 0.01.

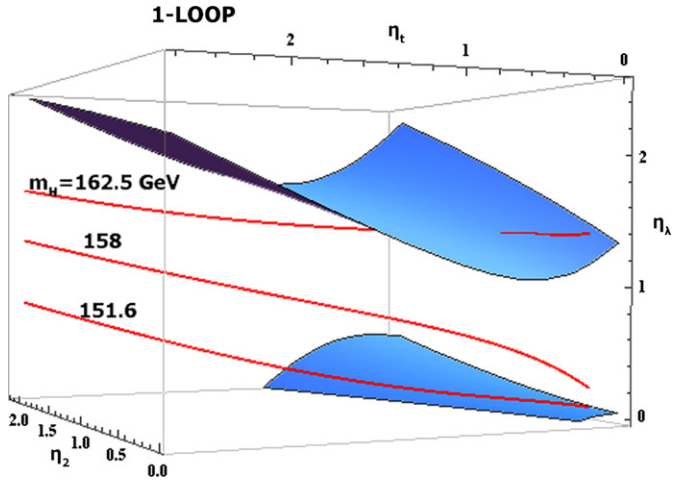

Fig. 3. Surfaces of constant η_λ and parametric curves of $(\eta_2(t), \eta_t(t), \eta_\lambda(t))$ for three values of the Higgs mass (1-loop).

to zero for very high energies). Then $F_{\eta_\lambda}(0, 0, \eta_\lambda)$ is just a second order polynomial in η_λ with zeros at ~ 1.34 and ~ 0.047, which are the two fixed points observed many years ago [6]. We can plot, in the space of $(\eta_2, \eta_t, \eta_\lambda)$, the surface where $F_{\eta_\lambda}(\eta_2, \eta_t, \eta_\lambda) = 0$. We can also numerically solve the differential equation and express η_λ as a function of t. Then we can make a parametric plot of the curve $(\eta_2(t), \eta_t(t), \eta_\lambda(t))$. We expect that for high energies, i.e. low values of η_2 and η_t, the curve will lie on the surface $F_{\eta_\lambda} = 0$. This is shown in Fig. 3. There are two surfaces corresponding to $F_{\eta_\lambda} = 0$ and we have plotted the parametric curves for three Higgs masses. We clearly see that for the values $m_H \sim 162.5$ and 151.6 GeV, the parametric curves lie on the surfaces for low values of η_2 and η_t.

3. The reduction equations

The observations made in Section 2 suggest that the couplings $\tilde{\lambda}$ and α_1 at least, are not independent in the SM and there

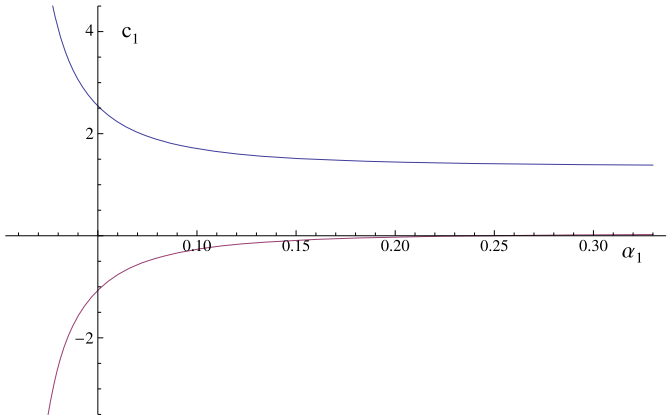

Fig. 4. The "constant" c_1 as a function of α_1.

may exist a functional relation among them at high scales. It is therefore justified to look for solutions of the reduction equation

$$\frac{d\tilde{\lambda}}{d\alpha_1} = \frac{\beta_\lambda}{\beta_1}. \tag{7}$$

Let us first look for solutions of Eq. (6) at one loop using the ansatz

$$\lambda(t) = c_1 \alpha_1(t), \tag{8}$$

where c_1 would be a constant in the perturbative approach of Ref. [1–5,8,9,11], but here we are searching for more general solutions. Taking the 1-loop expression for $\alpha_1(t)$ we can solve for t and express $\alpha_2(t)$ and $\alpha_t(t)$ (which are present in β_λ) as functions of α_1. Using the ansatz given in Eq. (8), Eq. (7) becomes a second order polynomial in c_1, where, of course, the coefficients depend on α_1. In Fig. 4 we plot the two roots of the polynomial as functions of α_1. We clearly see that for large values of α_1 (i.e. large energies), the two roots tend to constant values. This is easily understood, since for high energies, we can neglect all the couplings but α_1 itself, and Eq. (7) reduces to

$$c_1 = \frac{L_2 \alpha_1^2 c_1^2 + c_1 A_{1L} \alpha_1^2 + A_{11} \alpha_1^2}{b_1 \alpha_1^2} = \frac{L_2 c_1^2 + c_1 A_{1L} + A_{11}}{b_1} \tag{9}$$

and the two roots become independent of α_1 (1.34233 and 0.0465609 respectively). We have already encountered this behavior when examining Eq. (6). The second order polynomial above is essentially $F_{\eta_\lambda}(0, 0, \eta_\lambda)$. It is worth mentioning that the values of α_1, when c_1 approaches one of its fixed points correspond to energies well above the Planck scale. (At the Planck scale $\alpha_1 \sim 0.017$!)

We can go one step further and postulate that

$$\eta_\lambda = \frac{\tilde{\lambda}}{\alpha_1} = c_1 + c_2(\eta_2). \tag{10}$$

For high energies, the ratio η_2 tends to zero and in order to obtain our first ansatz, we must require that $c_2(\eta_2 \to 0) = 0$. From Eqs. (10) and (3) we easily get

$$\frac{dc_2}{dt} = \frac{d\eta_\lambda}{dt} = \alpha_1 \beta_\lambda(1, \eta_2, \eta_t, \eta_\lambda) - \alpha_1 \eta_\lambda b_1. \tag{11}$$

Writing

$$\frac{d\eta_2}{dt} = \frac{1}{\alpha_1}\frac{d\alpha_2}{dt} - \frac{\alpha_2}{\alpha_1^2}\frac{d\alpha_1}{dt} = \alpha_1\left(b_2 \eta_2^2 - \eta_2 b_1\right), \tag{12}$$

where b_2 is the one loop β-function coefficient for α_2; dividing the last two equations we get the derivative of c_2 with respect to η_2.

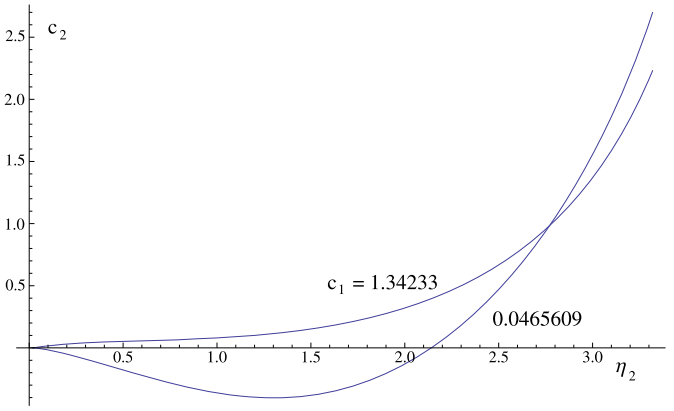

Fig. 5. Plotting c_2 as a function of η_2 for the two values of c_1 (1-loop).

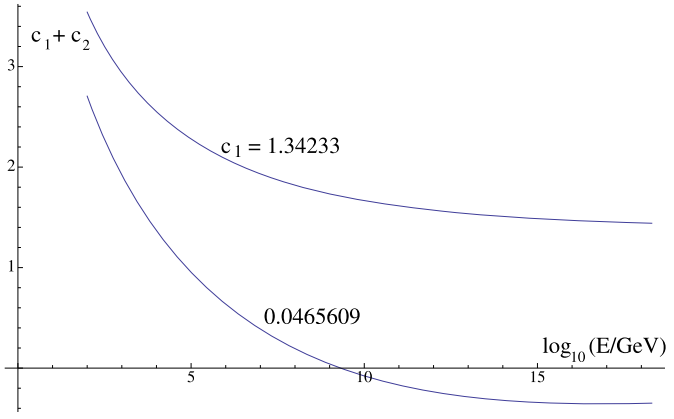

Fig. 6. Plotting $c_1 + c_2 = \eta_\lambda$ as a function of $\log_{10}(E)$ for the two values of c_1 (1-loop).

All that remains to be done is to express the ratio η_t as a function of η_2. Having the 1-loop analytical expressions for α_t and α_1 as functions of t, we can substitute t from the relation

$$\eta_2 = \frac{\alpha_2}{\alpha_1} = \frac{\frac{\alpha_{20}}{1-\frac{b_2}{2\pi}\alpha_{20}(t-t_0)}}{\frac{\alpha_{10}}{1-\frac{b_1}{2\pi}\alpha_{10}(t-t_0)}} \quad \rightarrow$$

$$t = t_0 + \frac{\eta_{20} - \eta_2}{\frac{1}{2\pi}[\eta_0 b_1 \alpha_{10} - \eta_2 b_2 \alpha_{20}]}, \tag{13}$$

where $\eta_{20} = \alpha_{20}/\alpha_{10}$ and α_{10} and α_{20} are the corresponding values at the scale t_0. Substituting $\eta_\lambda = c_1 + c_2(\eta_2)$ and solving the differential equation for $c_2(\eta_2)$, we get $c_2(\eta_2)$. In Fig. 5 we show the solutions for the two choices of c_1 using the initial condition $c_2(\eta_2 = 0.2) = 0$ (see Fig. 4). In Fig. 6 we show $c_1 + c_2$ (i.e. η_λ) as a function of the energy scale. The curve which corresponds to the higher c_1 value has almost reached that value at the Planck scale, while the one that corresponds to the lower c_1 value, apart from passing through unacceptable negative values, is still far away from that value. In Fig. 7 we plot the function $(c_1 + c_2(t))\alpha_1(t)$, i.e. $\tilde{\lambda}(t)$ itself, for the higher c_1 value curve. The corresponding running (pole[3]) Higgs mass is $\sim 162(154)$ GeV.

Going to 2-loop order, we should first determine the value(s) of the constant c_1 in Eq. (8). In this order, the procedure of keeping only the large terms in the high-energy regime, does not lead to

[3] For the known value of the top mass and the specific region of the Higgs mass, the Higgs pole mass is lower than the running mass by an amount of ~ 4.6–4.7%. The relation between running and pole mass can be found in Ref. [14].

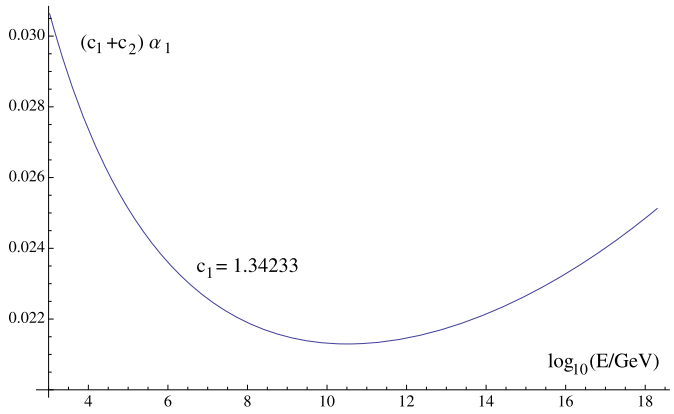

Fig. 7. Plotting $(c_1 + c_2)\alpha_1 = \tilde{\lambda}$ as a function of $\log_{10}(E)$ for the higher value of c_1. The corresponding running Higgs mass is ~ 162 GeV (1-loop).

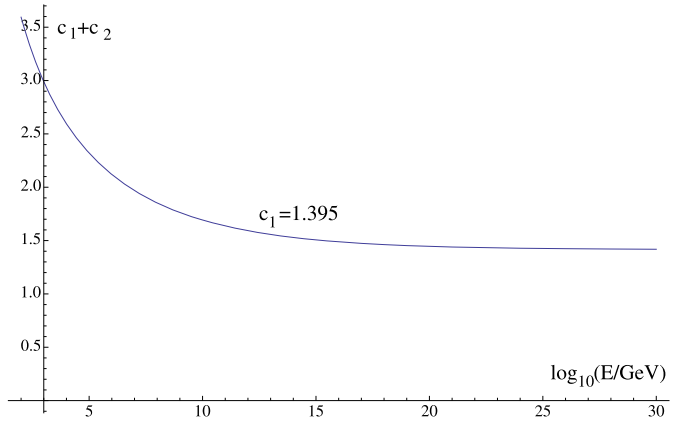

Fig. 8. Plotting η_λ as a function of $\log_{10}(E)$ for $c_1 = 1.395$. The corresponding running (pole) Higgs mas is ~ 163 (155) GeV (2-loop running).

an independent of α_1 value(s) c_1. Nevertheless, for a wide range of α_1, c_1 varies by less than 5% from its 1-loop values: 0.0448–0.0465 for the lower value and 1.342–1.395 for the higher one. We may now solve the 2-loop differential equation for c_2 using as initial value of η_λ at (very) high energies (i.e. low value of η_2) $c_1 = 1.395$. The new value drives the ratio η_λ to its constant value early on the energy scale (see Fig. 8). To be more specific, we see that $\eta_\lambda(M_{Planck}) = 1.459$ and it remains pretty stable for higher energies. The Higgs running (pole) mass is ~ 163 (155) GeV. At the 2-loop level, the problem with the lower c_1 value persists: η_λ passes through negative values.

4. The MSSM case

If we assume that the top and bottom Yukawa couplings are related, the reduction equation is

$$\frac{d\alpha_t}{d\alpha_b} = \frac{\beta_t}{\beta_b} = \frac{\alpha_t(6\alpha_t + \alpha_b - c_i^{(t)}\alpha_i)}{\alpha_b(6\alpha_b + \alpha_t + \alpha_\tau - c_i^{(b)}\alpha_i)},$$

where $c_i^{(t)} = (13/15, 3, 16/3)$ and $c_i^{(b)} = (7/15, 3, 16/3)$. Let us ignore, for simplicity, the contribution of α_τ and the small difference between $c_1^{(t)}$ and $c_1^{(b)}$. It is then straightforward to deduce that if the ratio α_t/α_b is constant, this ratio is equal to the corresponding ratio of the β-functions and equals 1.

$$\frac{d}{dt}\left(\frac{\alpha_t}{\alpha_b}\right) = 0 \quad \rightarrow \quad \frac{1}{\alpha_b^2}(\alpha_b\beta_t - \alpha_t\beta_b) = 0 \quad \rightarrow \quad \frac{\alpha_t}{\alpha_b} = \frac{\beta_t}{\beta_b}.$$

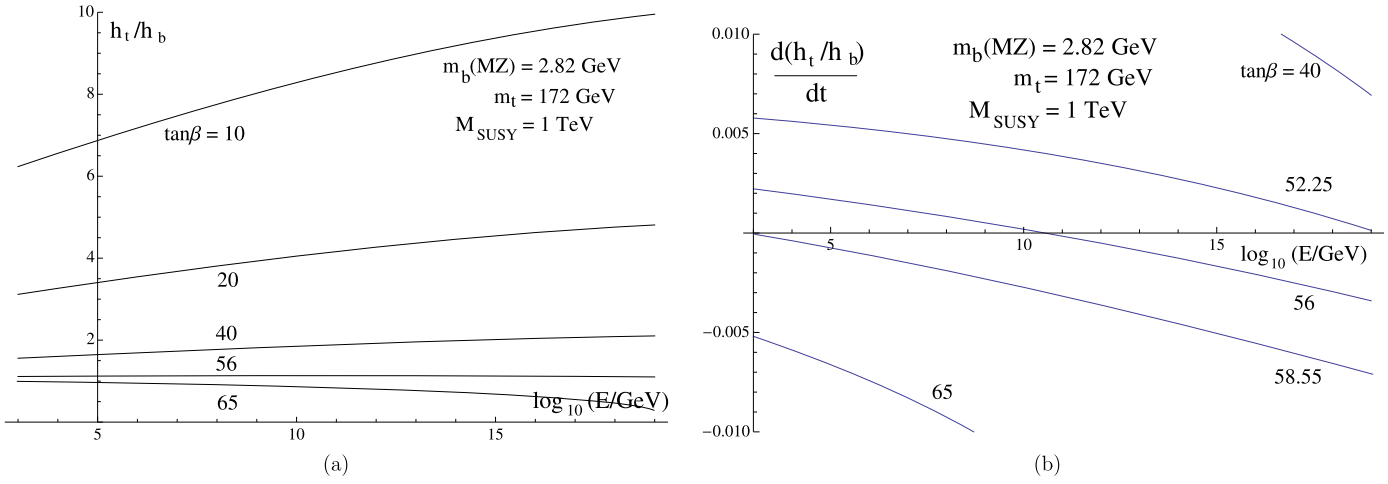

Fig. 9. (a) The ratio h_t/h_b and (b) the derivative of the ratio as a function of energy for several values of $\tan\beta$ and $M_{SUSY} = 1$ TeV, $m_t = 172$ GeV and $m_b(M_Z) = 2.82$ GeV.

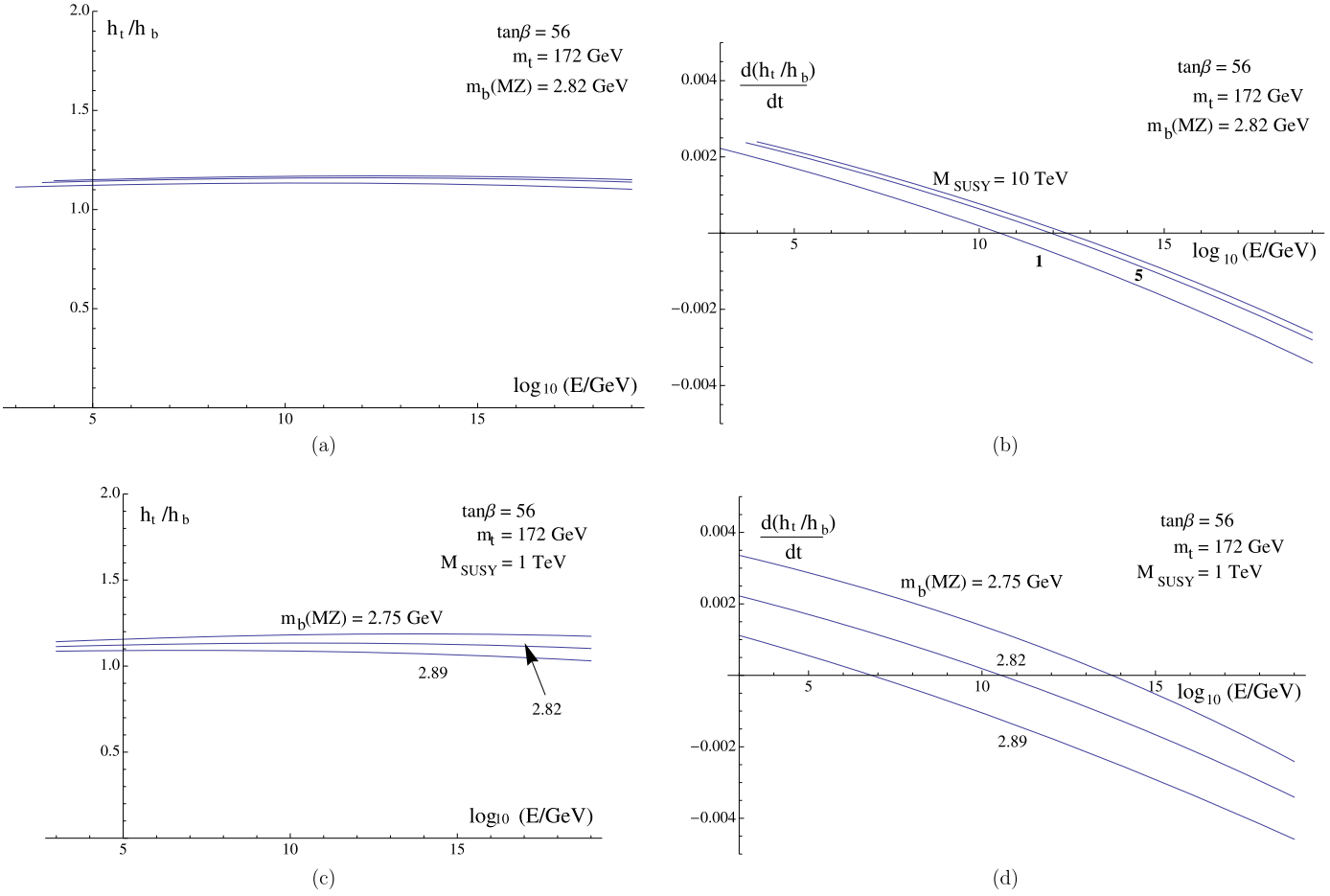

Fig. 10. Plots of the ratio h_t/h_b ((a) and (c)) as well as the derivative of the ratio ((b) and (d)) as a function of energy for $M_{SUSY} = 1$, 5 and 10 TeV ((a) and (b)) and varying the bottom mass in the experimental error region ((c) and (d)).

This result combined with the previous equation leads to

$$6\alpha_t + \alpha_b - c_i^{(t)}\alpha_i = 6\alpha_b + \alpha_t + \alpha_\tau - c_i^{(b)}\alpha_i \quad \rightarrow \quad \alpha_t = \alpha_b.$$

That is, if we start with α_t and α_b equal at an energy scale, equality will persist at all energies. Putting back the τ Yukawa coupling and the difference between the $c_1^{(t)}$ and $c_1^{(b)}$ constants, we expect a small deviation from that behavior.

Thus, the procedure goes as follows: we start the running (with the SM RGEs) from the known values of the top-, bottom- and tau-mass. At M_{SUSY}, we choose the appropriate $\tan\beta$ value that keeps the ratio α_t/α_b constant for all energies. Of course, we expect[4] this constant to be near 1.

[4] The fact that $\tan\beta$ could be predicted using reduction of couplings was suggested in [4] in a discussion with a different focus.

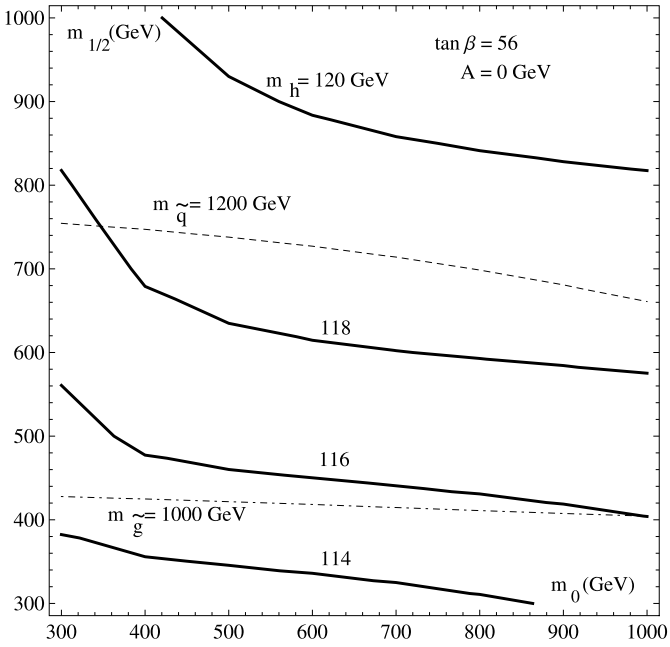

Fig. 11. Contours of constant m_h (pole) mass in the plane of $(m_0, m_{1/2})$ for initial value $A = 0$ GeV and for $\tan\beta = 56$. The dashed and the dotted–dashed contours correspond to (lightest) squark and gluino masses of 1.2 TeV and 1 TeV correspondingly.

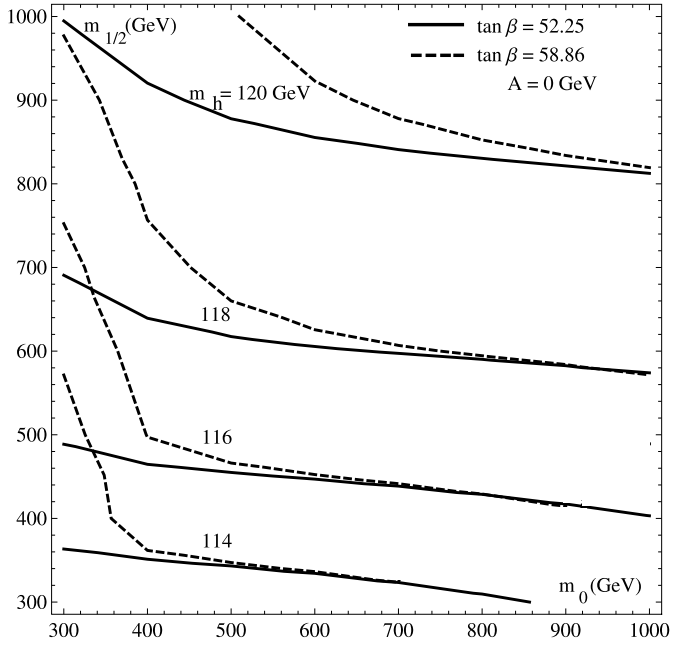

Fig. 12. The same as in Fig. 11 for the two limiting $\tan\beta$ cases: 58.55 and 52.25.

In the MSSM scenario, at the scale M_{SUSY}, we have the relations

$$\alpha_t(SM) = \alpha_t(MSSM)\sin^2\beta,$$
$$\alpha_b(SM) = \alpha_b(MSSM)\cos^2\beta,$$
$$\alpha_\tau(SM) = \alpha_\tau(MSSM)\cos^2\beta. \tag{14}$$

Above the M_{SUSY} scale, the running of all the parameters obeys the MSSM renormalization group equations, while below that scale, the SM regime is active.

In Fig. 9 we plot the ratio h_t/h_b (a) and the derivative of the ratio (b) as a function of energy, for several values of $\tan\beta$ and $M_{SUSY} = 1$ TeV, $m_t = 172$ GeV and $m_b(M_Z) = 2.82$ GeV. We clearly see that in the range $\tan\beta = 52.25$–58.55, the derivative of the ratio almost vanishes (actually it is less than $6 \cdot 10^{-3}$). The two values of $\tan\beta$: 52.25 and 58.55, are the limiting cases. For values below the first one, the derivative remains positive, while above the second one the derivative remains negative for the whole energy range.

In Fig. 10 we plot the ratio h_t/h_b (in (a) and (c)) as well as the derivative of the ratio (in (b) and (d)) as a function of energy for the central value of $\tan\beta = 56$. In (a) and (b) we show three curves corresponding to $M_{SUSY} = 1$, 5 and 10 TeV, keeping the masses of the top and bottom quarks at their central values. In (c) and (d) we vary the bottom mass $m_b(M_Z) = 2.75$, 2.82 and 2.89 GeV, keeping the top mass at its central value and $M_{SUSY} = 1$ TeV. The differences upon varying the top mass are negligible.

Now, using SUSPECT [15],[5] we can plot in the $(m_0, m_{1/2})$ plane contours of constant (pole) mass values for the lightest supersymmetric Higgs m_h[6] for $\tan\beta = 56$. In Fig. 11 we show these contours for $m_h = 114, 116, 118, 120$ GeV for initial $A = 0$ GeV and $\tan\beta = 56$. The dotted-dashed contour corresponds to a gluino mass of 1 TeV, while the dashed contour to (the lightest) squark mass of 1.2 TeV. According to recent data from ATLAS/LHC and CMS/LHC [16], the two values represent the lower bounds for detection of the corresponding particle. Finally, in Fig. 12 we plot the same contours for the two limiting $\tan\beta$ cases: 58.55 and 52.25.

5. Conclusions

The idea of couplings reduction in a field theory is very appealing since it increases its predictive power. Successful reduction led to all-loop finite theories and a prediction for the top-quark mass. The latter property was used as a selection criterion for a successful GUT. In the present work, we have investigated the approximate reduction of α_1 and the scalar quartic coupling λ couplings that appears to hold in the SM and MSSM models. Under plausible assumptions we have obtained a prediction for the Higgs particle running (pole) mass: $\sim 163(155)$ GeV.

Previous studies have either overlooked this possibility, or did not include the heavy top-quark contribution. We have also initiated an analogous analysis for the MSSM, which we plan to extend in a forthcoming publication.

Acknowledgements

It is a pleasure to thank A. Djouadi, W. Hollik, S. Heinemeyer, L. Fayard, J. Kubo, E. Ma, M. Mondragon and W. Zimmermann for very interesting discussions. G.Z. is grateful to the Sommerfeld-LMU and MPI Munich for the warm hospitality. This work was partially supported by the NTUA basic research support program "PEVE" 2009 and 2010 and the European Union ITN programme "UNILHC" PITN-GA-2009-237920.

References

[1] D. Kapetanakis, M. Mondragon, G. Zoupanos, Z. Phys. C 60 (1993) 181, hep-ph/9210218;
M. Mondragon, G. Zoupanos, Nucl. Phys. Proc. Suppl. 37C (1995) 98;
For an extended discussion and a complete list of references see S. Heinemeyer, M. Mondragon, G. Zoupanos, SIGMA 6 (2010) 049, arXiv:1001.0428 [hep-ph].

[5] We run the program using the mSUGRA model, 2-loop running and evaluation of pole masses. In all cases $\text{sign}(\mu) = +1$.

[6] We keep m_H for the SM Higgs and denote by m_h the lightest Higgs in the MSSM.

[2] J. Kubo, M. Mondragon, G. Zoupanos, Nucl. Phys. B 424 (1994) 291.
[3] J. Kubo, M. Mondragon, N.D. Tracas, G. Zoupanos, Phys. Lett. B 342 (1995) 155, hep-th/9409003;
J. Kubo, M. Mondragon, S. Shoda, G. Zoupanos, Nucl. Phys. B 469 (1996) 3, hep-ph/9512258;
J. Kubo, M. Mondragon, G. Zoupanos, Phys. Lett. B 389 (1996) 523, hep-ph/9609218.
[4] J. Kubo, M. Mondragon, M. Olechowski, G. Zoupanos, Nucl. Phys. B 479 (1996) 25, hep-ph/9512435.
[5] W. Zimmermann, Commun. Math. Phys. 97 (1985) 211;
R. Oehme, W. Zimmermann, Commun. Math. Phys. 97 (1985) 569.
[6] E. Ma, Phys. Rev. D 17 (1978) 623;
E. Ma, Phys. Rev. D 31 (1985) 1143.
[7] N.P. Chang, Phys. Rev. D 10 (1974) 2706.
[8] S. Nandi, W.-C. Ng, Phys. Rev. D 20 (1979) 972.
[9] C. Lucchesi, O. Piguet, K. Sibold, Helv. Phys. Acta 61 (1988) 321;
C. Lucchesi, G. Zoupanos, Fortschr. Phys. 45 (1997) 129, hep-ph/9604216.
[10] A.V. Ermushev, D.I. Kazakov, O.V. Tarasov, Nucl. Phys. B 281 (1987) 72;
D.I. Kazakov, Mod. Phys. Lett. A 2 (1987) 663.
[11] J. Kubo, K. Sibold, W. Zimmermann, Nucl. Phys. B 259 (1985) 331.
[12] J. Iliopoulos, hep-ph/0603146;
B. Ananthanarayan, J. Pasupathy, Int. J. Mod. Phys. A 17 (2002) 335, hep-ph/0104286.
[13] ATLAS Note, ATLAS-CONF-2011-135, September 30, 2011;
CMS PAS HIG-11-022;
ATLAS and CMS Collaborations, Combined Standard Model Higgs boson searches with up to 2.3 fb^{-1} of pp collision data at $\mathrm{ps} = 7$ TeV at the LHC, ATLAS-CONF-2011-157, CMS PAS HIG-11-023;
G. Rolandi, Higgs status (Tevatron+LHC) and combinations, in: HadronCollider-Physics Symposium 2011, Paris, France;
P. Jenni, The LHC project and discovery physics, in: Proceedings of the Corfu Summer Institute, 2011, in press.
[14] B. Schrempp, M. Wimmer, Prog. Part. Nucl. Phys. 37 (1) (1996), hep-ph/9606386;
A. Sirlin, R. Zucchini, Nucl. Phys. B 266 (1986) 389;
J.A. Casas, J.R. Espinosa, M. Quiros, A. Riotto, Nucl. Phys. B 436 (1994) 209;
J.A. Casas, J.R. Espinosa, M. Quiros, A. Riotto, Nucl. Phys. B 439 (1995) 466 (Erratum).
[15] A. Djouadi, J.L. Kneur, G. Moultaka, SuSpect: a program for the calculation of the SUpersymmetric particle SPECTrum, hep-ph/0211331.
[16] A. De Roeck, LHC: Searches for new physics beyond the Standard Model, in: Proceedings of the Corfu Summer Institute, 2011, in press.